

Discrete localized modes supported by an inhomogeneous defocusing nonlinearity

Goran Gligorić¹, Aleksandra Maluckov¹, Ljupčo Hadžievski¹, and Boris A. Malomed²

¹ *P group, Vinča Institute of Nuclear Sciences, University of Belgrade, P. O. B. 522,11001 Belgrade, Serbia*

² *Department of Physical Electronics, School of Electrical Engineering, Faculty of Engineering, Tel Aviv University, Tel Aviv 69978, Israel*

We report that infinite and semi-infinite lattices with spatially inhomogeneous self-defocusing (SDF) onsite nonlinearity, whose strength increases rapidly enough toward the lattice periphery, support stable unstaggered (UnST) discrete bright solitons, which do not exist in lattices with the spatially uniform SDF nonlinearity. The UnST solitons coexist with stable staggered (ST) localized modes, which are always possible under the defocusing onsite nonlinearity. The results are obtained in a numerical form, and also by means of variational approximation (VA). In the semi-infinite (truncated) system, some solutions for the UnST surface solitons are produced in an exact form. On the contrary to surface discrete solitons in uniform truncated lattices, the threshold value of the norm vanishes for the UnST solitons in the present system. Stability regions for the novel UnST solitons are identified. The same results imply the existence of ST discrete solitons in lattices with the spatially growing self-focusing nonlinearity, where such solitons cannot exist either if the nonlinearity is homogeneous. In addition, a lattice with the uniform onsite SDF nonlinearity and exponentially decaying inter-site coupling is introduced and briefly considered too. Via a similar mechanism, it may also support UnST discrete solitons, under the action of the SDF nonlinearity. The results may be realized in arrayed optical waveguides and collisionally inhomogeneous Bose-Einstein condensates trapped in deep optical lattices. A generalization for a two-dimensional system is briefly considered too.

PACS numbers: 03.75.Lm; 05.45.Yv

I. INTRODUCTION

The studies of self-sustained localized modes (bright solitons) in various physical settings have demonstrated that they can be supported by the self-focusing nonlinearity [1], or, in the form of gap solitons, by the self-defocusing (SDF) nonlinearity combined with periodic linear potentials [2], or in systems where the nonlinearity periodically changes its magnitude, and even the sign, along the evolution variable or in the transverse directions [3], [4]. Guiding bright solitons by pure SDF nonlinearities, without the help of a linear potential, was considered obviously impossible, until it was recently demonstrated in Refs. [5]- [7] that this is possible if the strength of the local SDF nonlinearity grows fast enough in space from the center to periphery, as a function of the radial coordinate, r . The existence of bright solitons in this case is a consequence of the fact that the growth of the nonlinearity coefficient makes the underlying equations *nonlinearizable* for the decaying tails (hence, the superposition principle is not valid for them), i.e., it makes unnecessary placing the propagation constant of the soliton into the semi-infinite spectral gap of the linearized system, where SDF nonlinearities cannot support any self-localization. A similar spatially inhomogeneous setting may support bright solitons under the action of the nonlocal SDF nonlinearity [8]. Independently, in Ref. [9] it was demonstrated that the uniform SDF nonlinearity may support bright solitons in a more exotic model, where the local diffraction coefficient decays at $r \rightarrow \infty$. Although the latter model is not equivalent to those introduced in Refs. [5] and [6], the mechanisms supporting bright solitons in these “nonorthodox” settings are similar.

The main subject of the present work is a possibility to create bright discrete solitons in two distinct one-dimensional (1D) lattice settings with inhomogeneous SDF onsite nonlinearities. First is a discrete counterpart of the system introduced in Refs. [5, 6], which is based on the discrete nonlinear-Schrödinger (DNLS) /Gross-Pitaevskii equation for the field amplitude in optical media, or the mean-field wave function of a Bose-Einstein condensate (BEC). As reviewed in Ref. [4], spatially inhomogeneous nonlinearities can be realized in various ways in optics [10]. For example, in photorefractive materials (such as LiNbO₃) nonuniform doping with Cu or Fe, which provide for the two-photon resonance, may be used for this purpose [11]. In the BEC, spatially modulated nonlinearity can be created, via the Feshbach resonance, by nonuniform external fields [12, 13]. Our goal is to construct discrete localized modes, of both staggered (ST) and unstaggered (UnST) types, in this setting, and investigate their stability and dynamics. Only the former type exists and may be stable in discrete media with the SDF uniform onsite nonlinearity. Therefore, we chiefly focus on stable UnST localized modes, the existence of which is the most nontrivial finding. In fact, the staggering transformation makes these modes tantamount to ST ones in the lattice with the inhomogeneous focusing nonlinearity, which is a counter-intuitive result too, as such discrete solitons do not exist in uniform lattices [14].

The second setting is the semi-infinite lattice with the SDF inhomogeneous nonlinearity. This discrete system generically supports surface solitons of the ST type, similarly to the periodic truncated potentials in solid state

media, where staggered localized modes pinned to the surface were first realized as localized electronic modes (the Tamm states) in solid-state media [15], [16]. The self-trapping of light near the edge of a waveguide array with self-focusing nonlinearity can lead to the formation of discrete UnST surface solitons [17], [18], [19]. It has been found that the surface modes acquire novel properties, different from those of discrete solitons in infinite lattices, such as a threshold power (norm) necessary for the existence of the surface solitons, and a possibility of coexistence of two surface modes, stable and unstable ones, at the same power. Generally, the existence and stability of diverse localized surface modes in semi-infinite nonlinear lattices are the result of the interplay between the nonlinearity and discreteness of the array, on the one hand, and the presence of the edge in the lattice, on the other. In this context, our goal is to investigate a possibility to generate different types of surface bright discrete solitons, and analyze their stability and dynamical properties, in the case when the local SDF strength grows from the edge into the depth of the lattice. In this case too, we are chiefly interested in the surface modes of the UnST type, which are impossible at the edge of a uniform truncated lattice with the SDF onsite nonlinearity.

We also introduce and briefly consider a discrete counterpart of the above-mentioned model with the uniform SDF nonlinearity and decaying diffraction coefficient [9], which corresponds to the inter-site coupling constant in the lattice, exponentially decaying with the increase of the discrete coordinate, $|n|$. Unlike the continuous medium, where it is difficult to realize a decreasing diffraction coefficient, in the lattice it merely implies a gradually growing spacing between the sites, as the coupling constant depends on it exponentially. While this model is very different from the one with the growing onsite SDF nonlinearity, UnST solitons, which are impossible in the uniform setting, are supported in it by a similar mechanism.

The paper is organized as follows. In Section II the models are introduced. The existence and stability of the UnST and ST discrete solitons in the infinite inhomogeneous lattice are reported in Section III. In addition to numerical results, this section also presents a variational approximation (VA) developed in an analytical form. Numerical and analytical results, including particular exact solutions and the VA, for the UnST and ST surface solitons in the truncated lattice are reported in Section IV. The paper is concluded by Section V, where, in particular, we discuss a two-dimensional generalization of the system, and give some preliminary results for it too.

II. THE MODELS

A. The infinite lattice

We here introduce two 1D discrete models in the form of the DNLS equations in the infinite and semi-infinite lattices (waveguide arrays, in terms of optics). The SDF onsite nonlinearity is assumed to grow exponentially from the central site in both directions in the infinite lattice, and from the edge towards the bulk in the semi-infinite one. It is necessary to stress that the steep growth of the local nonlinearity does not imply that one should use, for instance, a steeply growing density of the dopants (in the optical realization of the system). Instead, it is enough to assume that the density is uniform across the lattice, but the detuning of the two-photon resonance is gradually reduced from large to small values by means of a slightly inhomogeneous mechanical stress, or by means of the Zeeman or Stark shift. In any case, this mode of the resonance adjustment strongly affects only the local nonlinearity, but does not introduce a conspicuous linear potential, hence effects of the nonlinearity modulation may be studied in the “pure” form [6].

It is commonly known that lattices with the homogeneous SDF nonlinearity, both infinite and semi-infinite ones, give rise to bright discrete solitons of the ST type, while UnST localized modes cannot be created in such lattices [14]. In comparison with the infinite lattice, the truncation introduces an effective repulsive potential for discrete solitons, which acts in the combination with the periodic (Peierls–Nabarro [20], [21]) potential induced by the lattice. As a result, ST surface solitons are created if their norm (power) exceeds a certain threshold value, at which the discreteness may overcome the repulsion from the surface. As we demonstrate below, properties of the ST discrete solitons, in the infinite and truncated lattices alike, are not affected dramatically by the spatial modulation of the nonlinearity, while it opens the way to the creation of a completely novel species of UnST discrete solitons.

The 1D discrete model that we consider here is based on the following DNLS equation with the exponentially growing onsite SDF nonlinearity for complex field amplitudes u_n :

$$i \frac{du_n}{dz} = -\frac{1}{2}(u_{n+1} + u_{n-1} - 2u_n) + e^{\alpha|n|} |u_n|^2 u_n, \quad (1)$$

where $\alpha \geq 0$ is the growth rate. Stationary solutions to Eqs. (1) with real propagation constant K are looked for as

$$u_n(z) = e^{iKz} U_n, \quad (2)$$

where real discrete function U_n obeys the following equation:

$$-(K+1)U_n = -\frac{1}{2}(U_{n+1} + U_{n-1}) + e^{\alpha|n|}U_n^3, \quad (3)$$

which can be derived from the Lagrangian,

$$L = \frac{1}{2} \sum_{n=-\infty}^{+\infty} \left[(K+1)U_n^2 - U_n U_{n+1} + \frac{1}{2}e^{\alpha|n|}U_n^4 \right]. \quad (4)$$

Note that Eq. (3) has an exact analytical solution, which is valid at

$$K < K_{\text{cutoff}} \equiv \cosh(\alpha/2) - 1, \quad (5)$$

for either $n > 0$ or $n < 0$ (but not at positive and negative values of n simultaneously, therefore it does not correspond to solitons):

$$(U_n)_{\text{exact}} = A_{\text{exact}}e^{-\alpha|n|/2}, \quad (6)$$

$$A_{\text{exact}}^2 = \cosh(\alpha/2) - 1 - K. \quad (7)$$

In fact, this solution represents the above-mentioned *nonlinearizable tail* of the discrete solitons. On the other hand, for large α and/or large $-K$, the UnST soliton is strongly squeezed around $n = 0$, and can be described by the following truncated approximation:

$$U_0 \approx \sqrt{-(K+1)}, U_{\pm 1} \approx \left(-\frac{K+1}{4}\right)^{1/6} e^{-\alpha/3}, U_{\pm 2} \approx \left(-\frac{K+1}{2^8}\right)^{1/18} e^{-7\alpha/9}, \quad (8)$$

which is valid (for $K+1 < 0$) under the condition of

$$-(K+1)e^\alpha \gg 1. \quad (9)$$

It is worthy to note that, in the continuum counterpart of Eq. (3), with $U_{n+1} + U_{n-1} - 2U_n$ replaced by d^2U/dx^2 (x is the continuous coordinate), taking the equation at the inflexion point, where $d^2U/dx^2 = 0$ (obviously, any continuum-soliton profile features such a point), proves that the solitons may only exist with $K < 0$ [6]. Although this proof does not apply to the discrete model, the actual result is that the discrete UnST solitons too exist only at $K < 0$, see Eq. (31) and Fig. 5(b) below.

B. The semi-infinite lattice

In the truncated (semi-infinite) version of the model, Eq. (1) is modified as follows:

$$i\frac{du_n}{dz} = -\frac{1}{2}(u_{n+1} + u_{n-1} - 2u_n) + e^{\alpha|n|}|u_n|^2 u_n, \text{ at } n \geq 2, \quad (10)$$

$$i\frac{du_1}{dz} = -\frac{1}{2}(u_2 + C_0 u_0 - 2u_1) + e^\alpha |u_1|^2 u_1, \text{ at } n = 1, \quad (11)$$

$$i\frac{du_0}{dz} = -\frac{1}{2}C_0 u_1 + u_0 + \sigma_0 |u_0|^2 u_0, \text{ at } n = 0. \quad (12)$$

It is assumed here that the edge site of the semi-infinite lattice is labeled by $n = 0$, while the nonlinearity at this site may be different from that in the bulk ($\sigma_0 \neq 1$), and the coefficient of the inter-site coupling between the edge and the rest of the lattice may be different too from its bulk counterpart (which is scaled to be 1), i.e., $C_0 \neq 1$ in the general case.

The substitution of expression (2) transforms Eqs. (10)-(12) into the stationary form,

$$-(K+1)U_n = -\frac{1}{2}(U_{n+1} + U_{n-1}) + e^{\alpha|n|}U_n^3, \text{ at } n \geq 2, \quad (13)$$

$$-(K+1)U_1 = -\frac{1}{2}(U_2 + C_0 U_0) + e^\alpha U_1^3, \text{ at } n = 1, \quad (14)$$

$$-(K+1)U_0 = -\frac{1}{2}C_0 U_1 + \sigma_0 U_0^3, \text{ at } n = 0. \quad (15)$$

Under condition (9), these equations give rise to the same approximate (strongly squeezed) solution as given by Eq. (8), with a difference that components U_{-1} and U_{-2} are absent.

Equations (13)-(15) can be derived from the respective Lagrangian, cf. Eq. (4),

$$L = \frac{1}{2} \left\{ \sum_{n=1}^{\infty} \left[(K+1)U_n^2 - U_n U_{n+1} + \frac{1}{2} e^{\alpha n} U_n^4 \right] + (K+1)U_0^2 - C_0 U_0 U_1 + \frac{\sigma_0}{2} U_0^4 \right\}, \quad (16)$$

The total power (norm) of the modes in the infinite and truncated lattices is defined, respectively, as

$$P_{\text{infin}} = \sum_{n=-\infty}^{+\infty} U_n^2, \quad P_{\text{trunc}} = \sum_{n=0}^{+\infty} U_n^2. \quad (17)$$

It is relevant to mention that obvious rescaling,

$$(U_n)_{\text{infin}} \equiv \text{sign}(n) \cdot e^{\alpha/2} (U_{|n|-1})_{\text{trunc}}, \quad \text{for } |n| \geq 1, \quad (18)$$

and $(U_0)_{\text{infin}} = 0$, of discrete solitons found in the truncated lattice with $C_0 = \sigma_0 = 1$ yields odd (alias "twisted" [14, 22]) soliton modes in the infinite lattice.

As said above, our objective is to use the inhomogeneous SDF nonlinearity for creating stable discrete localized modes, both in the bulk and at the surface, as suggested by the analysis recently reported for continuous models [6]. In most cases, such modes, both fundamental and topological ones (multipoles and vortices) are stable, and unstable ones transform into tightly confined breathers.

The bright solitons in the continuous models were found also with the growth rate of the nonlinearity slower than exponential. The necessary and sufficient condition for supporting solitons with a finite norm by the SDF nonlinearity in the D -dimensional continuous space is that the nonlinearity coefficient in front of the cubic term, $g(r)$ [such as $e^{\alpha|n|}$ in Eq. (1)], must grow with the distance from the center, r , faster than r^D :

$$\lim_{r \rightarrow \infty} [r^D/g(r)] = 0. \quad (19)$$

The same condition remains true in discrete systems with the growing SDF nonlinearity, because the condition is determined by the asymptotic form of the solution far from the center, where the discrete medium seems as a quasi-continuum. Furthermore, condition (19) suggests not only the existence of the normalizable self-trapped modes, but also the fact that they may realize the ground state of the system, for given norm P . Indeed, the energy (Hamiltonian H) of such modes is obviously positive, while a competing trivial state, which might presumably give rise to $H = 0$, thus demonstrating that the self-trapped modes do not represent the ground state, may be taken as a delocalized distribution with radius $R \rightarrow \infty$ and vanishing density

$$U_{\text{deloc}}^2 = \alpha_D^{-1} R^{-D} P, \quad (20)$$

where the volume coefficient is $\alpha_1 = 2$, $\alpha_2 = \pi$, and $\alpha_3 = (4/3)\pi$. The corresponding quartic term in the Hamiltonian density is $h_{\text{quart}} = (1/2)g(r)U_{\text{deloc}}^4$, giving rise to a term in H which is estimated as

$$H_{\text{quart}}^{(\text{deloc})} = \frac{\alpha_D}{4} U_{\text{deloc}}^4 \int_0^R g(r) r^{D-1} dr. \quad (21)$$

Finally, the substitution of Eq. (20) into this expression demonstrates that $H_{\text{quart}}^{(\text{deloc})}$ *diverges* in the limit of $R \rightarrow \infty$ exactly in the case when condition (19) holds, hence the delocalized state cannot compete with the self-trapped one in the selection of the ground state.

The advantage of using the exponential modulation is a possibility to find particular solutions in an exact analytical form, and accurate results produced in this case by the VA [5, 7]. Therefore, here too we consider the model with the exponentially modulated nonlinearity, as already fixed in Eqs. (1) and (10). Both particular exact solutions and VA-based predictions are produced below. On the other hand, it is relevant to stress that the results are definitely structurally stable against a change of the particular form of the nonlinearity modulation, the only condition being that its local strength must not grow slower than prescribed by Eq. (19).

C. The lattice with the exponentially decaying coupling constant

Let us briefly mention the other possibility to obtain UnST solitons in the lattices with SDF nonlinearity. These lattices are characterized by the uniform SDF onsite nonlinearity and exponentially decreasing constant of the inter-site coupling. The model equations can be derived from the following Lagrangian of the inter-site coupling, cf. Eqs. (4) and (16):

$$L_{\text{coupl}}^{(\text{exp-decay})} = \frac{1}{2} \sum_n \left(e^{-\alpha|n-1|} u_n^* u_{n-1} + e^{-\alpha|n|} u_n^* u_{n+1} \right). \quad (22)$$

The respective DNLS equation for stationary solutions, sought for in the form of Eq. (2), is

$$-KU_n = -\frac{1}{2} \left(e^{-\alpha|n-1|} U_{n-1} + e^{-\alpha|n|} U_{n+1} \right) + U_n^3. \quad (23)$$

In particular, Eq. (23) admits an exact UnST exponential solution, which, as well as its counterpart (6) considered above, does not represent a soliton, and is a less generic solution, as it can be found in the exact form solely for $K = 0$:

$$K = 0, \quad U_n = \tilde{A}_{\text{exact}} e^{-\alpha|n|/2}, \quad (24)$$

$$\left(\tilde{A}_{\text{exact}} \right)^2 = e^{\alpha/2} \cosh(\alpha). \quad (25)$$

This result can be used to construct an exact solution for a discrete UnST soliton pinned to the edge to the truncated version of the present lattice, occupying the region of $n \geq 0$, with an ‘‘anomaly’’, accounted for by coefficient $C_0 \neq 1$, in the constant of the coupling between the edge site, $n = 0$, and the neighboring one, $n = 1$, cf. Eqs. (11) and (12) [unlike Eq. (12), we here assume that the onsite nonlinearity is completely uniform, i.e., $\sigma_0 \equiv 1$]. A simple analysis shows that the exact solution for the pinned soliton is given by Eqs. (24) and (25) at $n > 0$, while

$$U_0 = \left(C_0 \tilde{A}_{\text{exact}} / 2 \right)^{1/3} \quad (26)$$

at $n = 0$, provided that C_0 takes the special value,

$$C_0^4 = 2e^{\alpha/2} \cosh(\alpha). \quad (27)$$

Note that this value exceeds its bulk counterpart, $C_0 > (C_0)_{\text{bulk}} \equiv 1$.

For the truncated lattice with the exponentially growing onsite nonlinearity, which is described by Eqs. (10)-(12), a similar exact solution is given below, see Eqs. (34)-(37). Although such exact solutions are not generic ones, they provide the rigorous proof of the existence of the UnST discrete solitons in the lattices with the SDF nonlinearity, where solitons of this type cannot normally exist.

III. THE INFINITE LATTICE

A. Numerical results

For the numerical solution of the stationary equations, Eqs. (3) and (13)-(15), we adopted the nonlinear equation solver based on the Powell method [23]. Direct dynamical simulations of dynamical equations (1) and (10)-(12) were based on the Runge-Kutta numerical procedure of the sixth order.

It is well known that the lattice with the uniform onsite SDF nonlinearity supports stable bright solitons of the ST type, in onsite and inter-site configurations [14]. The ST soliton branches survive the change of the nonlinearity from uniform to exponentially modified, as in Eq. (1). Numerical calculations have shown that accordingly modified ST solitons, strongly pinned to the center of the lattice, can be found at all values of $\alpha > 0$, see Fig. 1(a). These discrete solitons are always stable.

Our main objective here is to demonstrate that the inhomogeneous onsite SDF nonlinearity supports stable UnST localized modes. In lattices with the uniform self-focusing nonlinearity, such solutions can be realized in two configurations with respect to the position of the soliton’s center, onsite and inter-site, i.e., centered on lattice site, or between two adjacent lattice sites, respectively. In the present model, the center of the UnST solitons naturally coincides with the minimum of the onsite nonlinearity strength (the bottom point of the U profile).

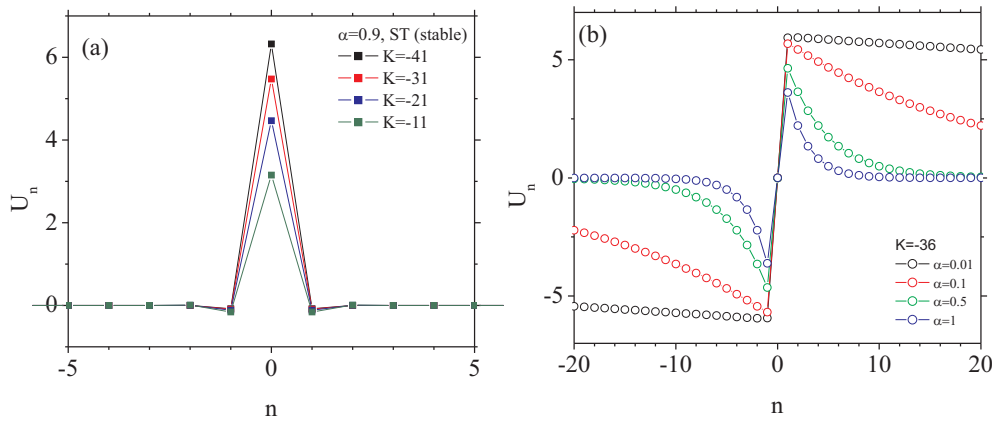


FIG. 1: (Color online) Profiles of stable staggered (a) and unstable twisted solitons (b), produced by the numerical calculations for parameters indicated in the figure.

In Figs. 2(a) and 2(b), dependencies of the total power on the propagation constant, and amplitude profiles are shown for UnST solitons at different values of steepness α of the nonlinearity-modulation profile in Eq. (1). Shapes of the modes for a fixed α and different values of propagation constant K are displayed in Fig. 2(c). In the lattice with the uniform onsite SDF nonlinearity, UnST localized modes do not exist (and, respectively, the uniform UnST background is not subject to the modulational instability). The exponential growth of the onsite nonlinearity strength from the center to periphery gives rise to UnST modes. At very small values of the growth rate, α , the mode seems as the background with a weak maximum at the lattice center, $n = 0$. The pinned UnST localized modes, with negligible tail amplitudes at the periphery of the modulated lattice, are found at $\alpha > \alpha_{\min} \approx 0.1$, when the exponential modulation is steep enough to trap the UnST soliton at the center, in the framework of the present numerical scheme.

The UnST soliton solutions have been found numerically at $\alpha < \alpha_{\max} \approx 1.5$. This limit is imposed by the numerical scheme, but not by the system per se [indeed, Eq. (8) demonstrates the existence of solutions at large values of α]. The linear-stability analysis predicts that the newly found UnST discrete solitons are chiefly stable in their existence region, except for a relatively narrow area shown in Fig. 3, where they are subject to an oscillatory instability.

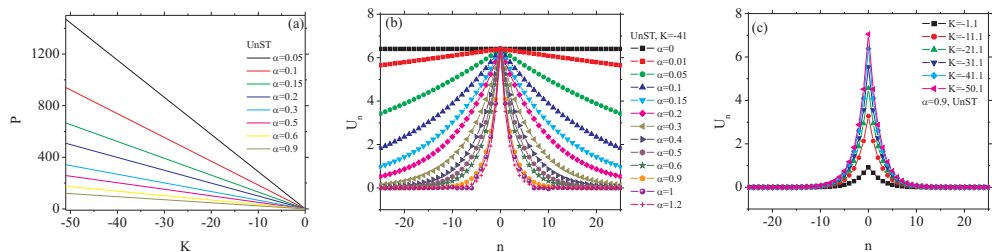


FIG. 2: (Color online) (a) The power versus the propagation constant for unstagere solitons. Plots (b) and (c) display shapes of the solitons. The respective values of α and K are indicated in the panels.

Direct simulations confirm the actual stability of the UnST solitons predicted by the linear-stability analysis, see Fig. 4(a). As concerns unstable solitons, they spontaneously evolve into confined irregularly oscillating breathers, as shown in Fig. 4(b). The internal frequency of the breather is determined by the imaginary part of the complex instability eigenvalues which govern the transformation of stationary solitons into the breathers.

As shown in Fig. 1(b), we have also found numerical solutions for the twisted soliton modes in the infinite lattice, with $U_{-n} = -U_{+n}$, which were introduced above by Eq. (18). They coexist with the UnST and ST solitons in the infinite lattice, but are always unstable, according to the linear stability analysis and direct simulations (unlike the stability of the similar solitons in the truncated lattice, see below). The simulations (not shown here in detail) demonstrate that the instability breaks the antisymmetry of those modes, as a consequence of a small oscillating field amplitude appearing at $n = 0$.

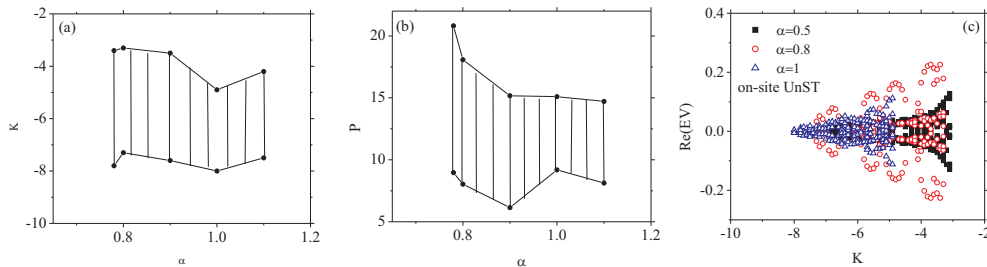


FIG. 3: The unstaggered solitons are subject to an oscillatory instability in the hatched areas, which are shown in the planes of (K, α) and (P, α) in plots (a) and (b), respectively. Examples of sets of real parts of complex eigenvalues (“EVs”) of perturbation modes are plotted versus K in (c). The instability is accounted for by $\text{Re}(\text{EV}) > 0$. Parameter values are indicated in the panels.

B. The variational approximation

The comparison with the continuous models elaborated in Refs. [6] and [7], as well as previous works dealing with discrete solitons in homogeneous nonlinear lattices [24–28], suggests that it may be relevant to develop a VA, based on the simple ansatz for the onsite-centered solution of the UnST type, which emulates the exact non-soliton solution (6):

$$U_n = A \exp\left(-\frac{\alpha}{2}|n|\right), \quad (28)$$

where A is treated as a variational parameter. The substitution of this ansatz into Lagrangian (4) easily leads to the corresponding effective Lagrangian:

$$L_{\text{eff}} = \frac{A^2}{2 \sinh(\alpha/2)} \left[\cosh(\alpha/2) \left(1 + K + \frac{1}{2}A^2 \right) - 1 \right]. \quad (29)$$

The variational equation, following from this Lagrangian, $\partial L_{\text{eff}}/\partial(A^2) = 0$, predicts the amplitude of the soliton,

$$A_{\text{VA}}^2 = -K - [1 - \text{sech}(\alpha/2)], \quad (30)$$

cf. Eq. (7). Note that Eq. (30) predicts a cutoff value of the propagation constant,

$$K_{\text{cutoff}}^{(\text{VA})} = -[1 - \text{sech}(\alpha/2)] < 0, \quad (31)$$

which is negative, unlike the positive cutoff produced by the exact non-soliton solution (6). Finally, the substitution of this result into expression for total power of ansatz (28),

$$P_{\text{ansatz}} = A^2 \coth(\alpha/2), \quad (32)$$

yields the prediction of the VA for the total power as a function of the propagation constant:

$$P_{\text{VA}} = -K \coth(\alpha/2) - \tanh(\alpha/4). \quad (33)$$

In Fig. 5(a), we compare, at different fixed values of α , the power-versus- K curves of the numerically generated UnST soliton families and their VA-predicted counterparts. It is seen that the agreement, quite naturally, improves, with the increase of the nonlinearity-modulation parameter α , for tighter self-trapped modes. Additionally, Fig. 5(b) compares the numerically found and VA-predicted [see Eq. (31)] cutoff values of the propagation constant at which the UnST-soliton branches originate.

IV. SURFACE SOLITONS IN TRUNCATED LATTICES

A. Exact solutions and the variational approximation

As mentioned above, a remarkable peculiarity of the truncated-lattice model, based on Eqs. (13)-(15), is a possibility to find particular solutions for surface solitons in an exact analytical form, which was not possible for the infinite lattice [recall the exact solution given by Eqs. (6) and (7) is not appropriate for solitons].

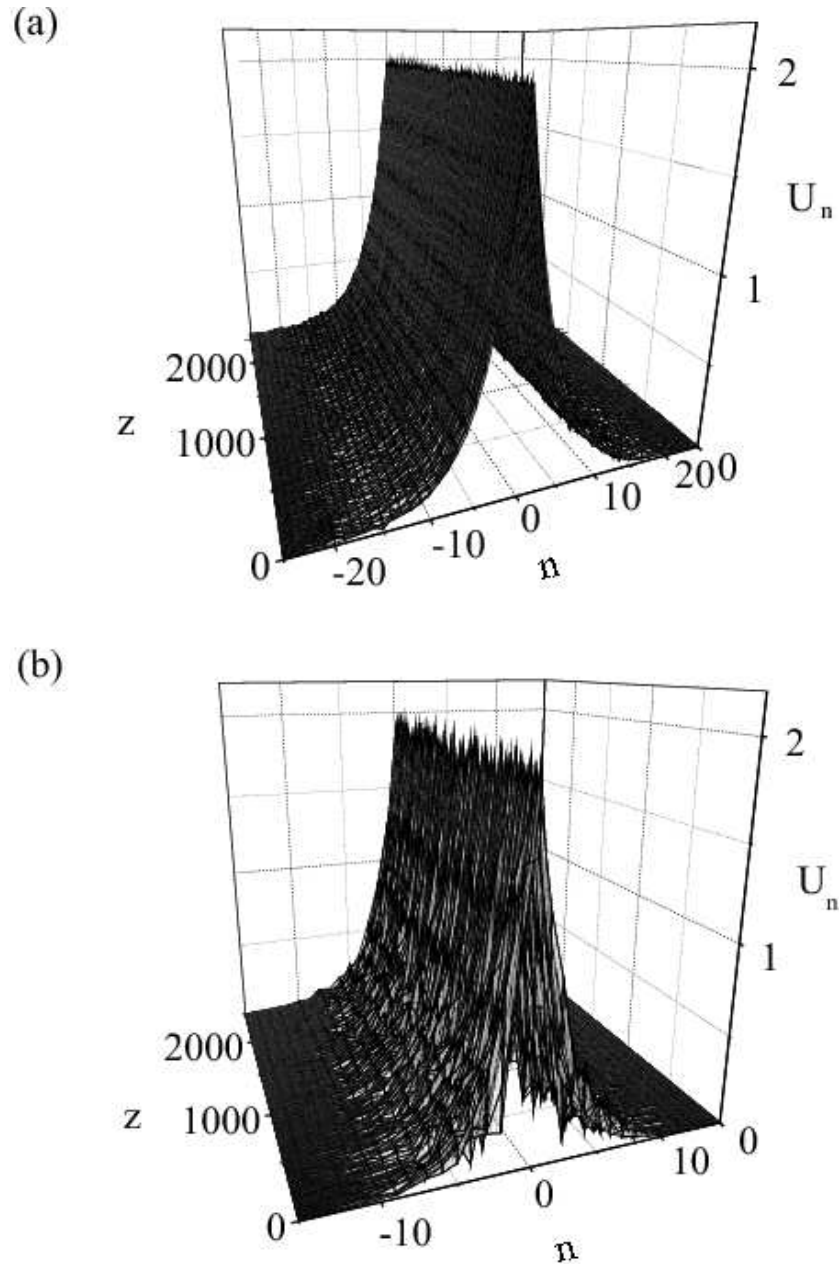


FIG. 4: The evolution of perturbed unstaggered solitons: (a) $\alpha = 0.5$, $K = -4$; (b) $\alpha = 1$, $K = -4$. The linear stability analysis predicts the stability for (a) and instability for (b).

1. The exact solution for unstaggered surface solitons

First, an exact solution for a UnST soliton pinned to the edge of the lattice is looked for as

$$\begin{aligned} U_n &= A \exp(-\alpha n/2), \text{ at } n \geq 1, \\ U_n &= U_0 \text{ at } n = 0, \end{aligned} \quad (34)$$

where U_0 may be different from A , cf. the exact solution for the model with the uniform onsite SDF nonlinearity and exponentially decaying inter-site couplings, given above by Eqs. (24)-(27). The substitution of ansatz (34) into Eqs. (13) and (14) yields the following relations:

$$K = \cosh(\alpha/2) - 1 - A^2. \quad (35)$$

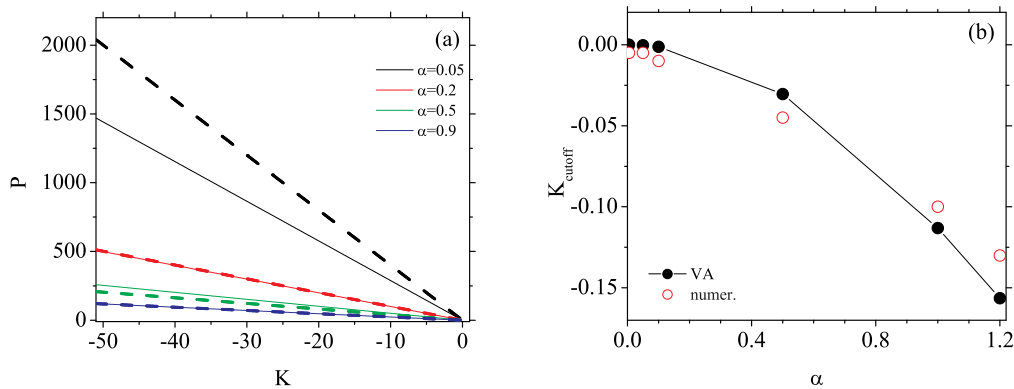


FIG. 5: (Color online) (a) The P vs. K dependencies for numerically found UnST solitons (solid lines), and their counterparts predicted by the VA (dashed lines), for fixed values of α indicated in the panel. (b) The corresponding cutoff values of K at which the soliton branches originate. Lines with filled circles depict the VA prediction given by Eq. (31), while hollow circles represent the numerical results.

$$U_0 = A/C_0. \quad (36)$$

Then, the substitution of the ansatz and relations (35), (36) into Eq. (15) yields the final result:

$$A^2 = \frac{C_0^2 e^{\alpha/2} + (1 - C_0^2) e^{-\alpha/2}}{2(C_0^2 - \sigma_0)}. \quad (37)$$

As usual, the exact solution is the exceptional one, which can be found with for the single value of the propagation constant, given by Eq. (35), like exceptional exact soliton solutions found in similar continuous models [6, 7]. Nevertheless, this exact solution is more generic than the above-mentioned one represented by Eqs. (24)-(26), because its existence does not require a special selection of the coupling constant C_0 , unlike condition (27)

The exact solution is meaningful if Eq. (37) yields $A^2 > 0$, i.e. C_0^2 belongs to either of the two intervals:

$$\sigma_0 < C_0^2 < 1 + e^\alpha, \quad \text{if } \sigma_0 < 1 + e^\alpha; \quad (38)$$

$$1 + e^\alpha < C_0^2 < \sigma_0, \quad \text{if } \sigma_0 > 1 + e^\alpha. \quad (39)$$

Note that the nonlinearity increases monotonously from the edge into the bulk of the lattice if condition $\sigma_0 < e^\alpha$ holds, which excludes the existence interval (39). In addition, in the absence of the “intersite-coupling anomaly”, i.e., for $C_0 = 1$, the remaining existence condition (38) implies that the nonlinearity at the edge site, $n = 0$, must be weaker than in the bulk: $\sigma_0 < 1$.

It is also relevant to mention that, in the same case of $C_0 = 1$, amplitude (37) of the exact solution never vanishes, in agreement with the fact that the total power of surface solitons, created in uniform truncated lattices, cannot be smaller than a finite threshold value [17]. On the other hand, admitting $C_0 > 1$ opens the way for vanishing of threshold: indeed, expression (37) vanishes at $C_0 = \sqrt{1 + e^\alpha}$.

2. The exact solution for staggered surface solitons

It is also possible to construct a particular exact solution to Eqs. (13)-(15) in the form of an ST soliton, although it turns out to be unstable, as shown below. We demonstrate this solution here for the sake of the completeness of the analysis.

The exact ST soliton is looked for as

$$\begin{aligned} U_n &= A(-1)^n \exp(-\alpha n/2), \quad \text{at } n \geq 1, \\ U_n &= U_0 \quad \text{at } n = 0, \end{aligned} \quad (40)$$

cf. Eq. (34). The substitution of this ansatz into the stationary equations leads to the following results for the exact solution, which replace Eqs. (35) and (37) obtained above for the UnST soliton:

$$K = -[\cosh(\alpha/2) + 1 + A^2], \quad (41)$$

$$A^2 = -\frac{C_0^2 e^{\alpha/2} + (1 - C_0^2) e^{-\alpha/2}}{2(C_0^2 - \sigma_0)}, \quad (42)$$

while relation (36) remains the same as before. As it follows from Eq. (42), the exact solution is meaningful (giving $A^2 > 0$) exactly in those regions where the above exact solution for the UnST soliton *does not* exist, cf. Eqs. (38) and (39). Being interested in the case of $\sigma_0 < e^\alpha$, when the strength of the onsite SDF grows monotonously from $n = 0$ towards $n \rightarrow \infty$, we finally conclude that the exact solution for the ST soliton exists at $C_0^2 < \sigma_0$. In particular, in the case of $C_0 = 1$ (no ‘‘coupling anomaly’’ at the surface), this solution exists under condition $\sigma_0 > 1$ (in fact, in interval $1 < \sigma_0 < e^\alpha$, according to what is said above), which is precisely opposite to the above-mentioned existence condition, $\sigma_0 < 1$, for the exact unstaggered solution, in the same case of $C_0 = 1$.

3. The variational approximation for unstaggered surface solitons

Because the existence of UnST solitons is the most essential feature of the model with the spatially modulated onsite SDF nonlinearity, and the above exact solution is available at the single value of the propagation constant, given by Eq. (35), it makes sense to apply the VA to the description of generic solutions for the UnST solitons. Recently, the VA was applied to discrete surface solitons in truncated lattices with the homogeneous onsite nonlinearity [27, 28].

We here aim to develop the VA for the surface solitons in the basic model with $C_0 = \sigma_0 = 1$, without ‘‘anomalies’’ at the edge of the lattice, when the corresponding Lagrangian (16) reduces to

$$L = \frac{1}{2} \sum_{n=0}^{\infty} \left[(K+1) U_n^2 - U_n U_{n+1} + \frac{1}{2} e^{\alpha n} U_n^4 \right]. \quad (43)$$

Essentially the same ansatz (28), as used above for discrete solitons in the infinite lattice,

$$U_n = A \exp(-(\alpha/2)n), \quad n \geq 0, \quad (44)$$

yields the following result, upon the substitution into Eq. (43):

$$L_{\text{eff}} = \frac{A^2}{4 \sinh(\alpha/2)} \left[\exp(\alpha/2) \left(1 + K + \frac{1}{2} A^2 \right) - 1 \right], \quad (45)$$

cf. Eq. (29). In the present case, the variational equation, $\partial L_{\text{eff}} / \partial (A^2) = 0$, yields

$$A_{\text{VA}}^2 = -[K+1 - \exp(-\alpha/2)], \quad (46)$$

cf. Eq. (30), with the respective cutoff at

$$K_{\text{cutoff}}^{(\text{surf-VA})} = -[1 - \exp(-\alpha/2)] < 0, \quad (47)$$

cf. Eq. (31). Finally, the total power of ansatz (44), $P_{\text{ansatz}}^{(\text{surf})} = A^2 [1 - \exp(-\alpha)]^{-1}$ [cf. Eq. (32)], yields the following prediction for the $P(K)$ curve for the family of UnST surface solitons:

$$P_{\text{VA}}^{(\text{surf})} = -K [1 - \exp(-\alpha)]^{-1} - [1 + \exp(-\alpha/2)]^{-1}, \quad (48)$$

cf. the result (33) predicted by the VA for the UnST solitons in the infinite lattice. Comparison of the analytical results for $P_{\text{VA}}^{(\text{surf})}$ and $K_{\text{cutoff}}^{(\text{surf-VA})}$, which are given by Eqs. (48) and (47), with the numerically obtained counterparts is presented in Figs. 6(c) and (d), respectively.

B. Numerical results

In the truncated lattice with the homogenous SDF nonlinearity, $\alpha = 0$, $\sigma_0 = \sigma = 1$, and uniform coupling between the lattice sites, $C_0 = 1$, the existence of two distinct families of discrete solitons of the ST type, pinned at the interface, one stable and one unstable, is well known (see, e.g., Ref. [17]). These solitons exist at the total power exceeding a finite threshold value, which is necessary for the lattice-pinning force to overcome the repulsion from the surface.

In the present model with the inhomogeneous nonlinearity, numerical results demonstrate that a nearly completely stable ST branch continues to exist for all values of α , C_0 , and σ , starting with a finite threshold power. These solitons are strongly pinned to the edge of the lattice, very weakly depending on the modulation steepness α , and are stable in their almost entire existence region. However, comparison of the numerically generated ST solitons with the exact solution given by Eqs. (40)-(42) demonstrates that the latter one and numerically found stable ST surface solitons belong to *different* solution branches. Accordingly, the linear-stability analysis shows that the exact solution is unstable (not shown here in detail).

The most essential numerical results concern the existence and stability of UnST solitons centered at the lattice surface. We have performed this analysis for various values of parameters C_0 and σ_0 , and for nonlinearity-modulation steepness taking values in the interval of $0 < \alpha < 1.5$, where stable UnST surface solitons can be found (as well as in the previous section, this limitation is imposed by the numerical scheme used, rather than by the system itself). The $P(K)$ curves for this family, and examples of solitons profiles are shown in Fig. 6. It is worthy to mention that the so found UnST surface solitons coexist with their numerically generated counterparts of the ST type in a broad parameter range, as shown in Fig. 7 for $\sigma_0 = 1$, $C_0 = 1.2$, and different values of α (recall that the particular exact analytical solutions for both types of the surface solitons do not coexist, as shown above).

A noteworthy novel property of the UnST solitons is vanishing of the threshold value of the total power necessary for their existence in the basic model $C_0 = \sigma_0 = 1$, see Fig. 6(c) and (d). This finding agrees with the variational results (46) and (47), which predict that the threshold is zero for the UnST solitons. The absence of the threshold has obvious implications for the physical realizations of the system, strongly facilitating the creation of the solitons.

Unlike the ST surface solitons, whose shape is almost independent of the nonlinearity-modulation rate α , the shape of the UnST solitons is quite sensitive to α . As illustrated in Fig. 7(c), in all cases when the particular exact solution for the UnST soliton, given by Eqs. (34)-(37), exists, it is identical to the numerical solution found at the same parameters (on the contrary to the above-mentioned case of the ST solitons, where the actually found stable numerical solutions and the unstable analytical one belong to different branches).

The numerical analysis demonstrates that the UnST surface solitons are stable almost everywhere in their existence region. The respective perturbation spectrum contains a small number of the complex eigenvalues with a finite real part only in a narrow area close to the existence threshold (not shown here in detail). Dynamical simulations of the perturbed evolution confirm the stability of the UnST solitons. In particular, the exact analytical soliton of the UnST type, which fits its numerical counterpart in Fig. 7 (b), is stable too.

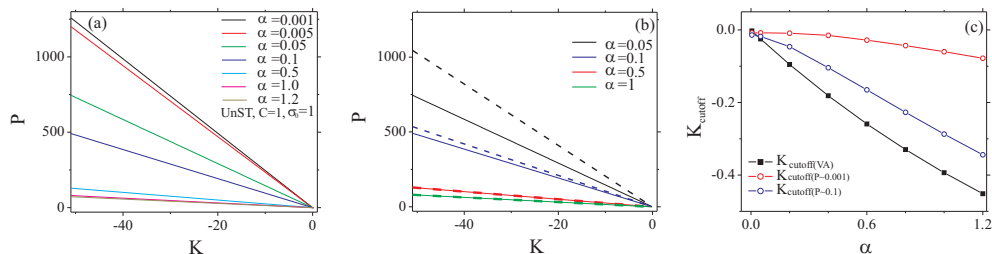


FIG. 6: (Color online) (a) The total power as a function of the propagation constant for unstaggregated surface solitons. In plot (b), numerically found $P(K)$ curves (solid lines) and their VA-predicted counterparts given by Eq. (48) (dashed lines) are compared for fixed values of α . Comparison of the prediction (47) for $K_{\text{cutoff}}^{\text{(surf-VA)}}$ with the corresponding numerically found cutoff value of the propagation constant is shown in (c). The red (upper) and blue (lower) curves corresponds to the cutoff defined by setting the total power of the numerically found surface solitons to $P_{\text{min}} = 0.001$ and $P_{\text{min}} = 0.1$, respectively. Here, parameters are $C_0 = 1$ and $\sigma_0 = 1$.

V. CONCLUSION AND EXTENSIONS

It is commonly known that the only localized modes in lattices with the homogeneous SDF (self-defocusing) nonlinearity are represented by ST (staggered) solitons. Here, we have demonstrated that infinite and semi-infinite (truncated) lattices support stable discrete UnST (unstaggregated) solitons too, provided that the strength of the onsite SDF nonlinearity grows rapidly enough from the center towards the periphery. The physical implementation of this setting may be provided by decreasing the detuning of the underlying resonance (the two-photon one in optics, or the Feshbach resonance in the BEC) in the same direction, from the center to periphery. Families of the UnST solitons have been found in the numerical form, and also reproduced by the VA (variational approximation). In addition to that, particular exact solutions were found for the UnST surface solitons in the semi-infinite lattice. Stability regions

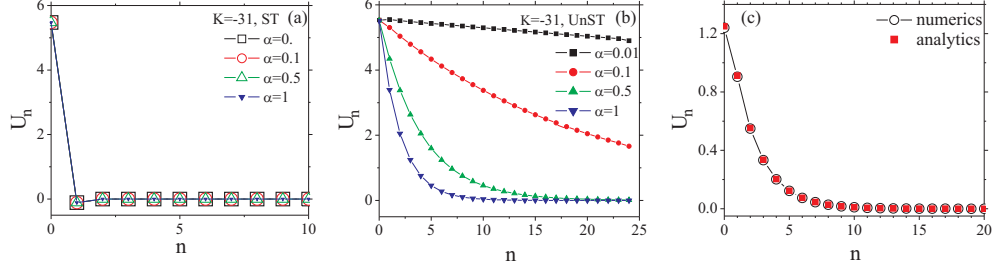


FIG. 7: (Color online) (a) and (b): Profiles of staggered (a) and unstaggered surface solitons (b), coexisting at $C_0 = 1.2$ and $\sigma_0 = 1$. Values of other parameters are indicated in the panels. (c) Profiles of the exact analytical solution for the unstaggered surface soliton and its numerically found counterpart (their coincidence verifies that the analytical and numerical solutions belong to the same branch), for $k = 1.13$, $C_0 = 1.2$, and $\sigma_0 = 1$.

for the UnST solitons have been found by means of the calculation of eigenvalues for perturbation modes, and verified by means of direct simulations. A noteworthy result is vanishing of the threshold value of the total power (norm) necessary for the existence of the surface UnST solitons in the truncated lattice. In both the infinite and truncated ones, the stable UnST solitons coexist with the (usual) stable ST-soliton families. The settings considered here may be implemented for matter waves in BEC trapped in deep optical lattices, and for light waves in arrays of optical waveguides. In addition to that, we have also introduced and briefly considered the lattice with the uniform SDF nonlinearity and exponentially decaying inter-site coupling. Physically, the latter feature can be readily provided by gradual increase of the lattice spacing. Discrete UnST solitons may exist in this system too, despite the SDF sign of the nonlinearity.

This work can be naturally extended in other directions. In particular, it may be interesting to study a similar system based on a set of two parallel linearly coupled lattices, i.e., a discrete nonlinear coupler, which is known in both infinite [25] and semi-infinite [28] forms.

A challenging problem is to generalize the analysis for two-dimensional (2D) lattices. In particular, a natural object may be a *corner-shaped* lattice (cf. Ref. [29]), with the SDF onsite nonlinearity modulated so that the stationary version of the 2D discrete nonlinear Schrödinger equation takes the following form [cf. Eq. (3)]:

$$\begin{aligned}
-(K+2)U_{m,n} &= -\frac{1}{2}(U_{m+1,n} + U_{m-1,n} + U_{m,n+1} + U_{m,n-1}) + \sigma e^{\alpha(m+n)}U_{m,n}^3, \text{ at } m, n \geq 1, \\
-(K+2)U_{m,0} &= -\frac{1}{2}(U_{m+1,0} + U_{m-1,0} + U_{m,1}) + \sigma_0 e^{\alpha m}U_{m,0}^3, \text{ at } m \geq 1, n = 0, \\
-(K+2)U_{0,n} &= -\frac{1}{2}(U_{0,n+1} + U_{0,n-1} + U_{1,n}) + \sigma_0 e^{\alpha n}U_{0,n}^3, \text{ at } n \geq 1, m = 0, \\
-(K+2)U_{0,0} &= -\frac{1}{2}(U_{1,0} + U_{0,1}) + \sigma_{00}U_{0,0}^3, \text{ at } m = n = 0.
\end{aligned} \tag{49}$$

It is assumed that linear couplings are uniform throughout the 2D lattice, but the nonlinearity coefficient may be modified near edges of the corner ($\sigma_0 \neq \sigma$), and additionally at the corner site ($\sigma \neq \sigma_{00} \neq \sigma_0$). Then, it is easy to demonstrate, as a proof of principle, that Eqs. (49) admit a particular exact solution for 2D UnST *corner soliton*:

$$U_{m,n} = A \exp\left(-\frac{\alpha}{2}(m+n)\right), \tag{50}$$

$$A^2 = (\sigma - \sigma_{00})^{-1} \exp\left(\frac{\alpha}{2}\right), \quad K = 2 \cosh\left(\frac{\alpha}{2}\right) - 2 - \sigma A^2, \tag{51}$$

under additional conditions

$$\sigma + \sigma_{00} = 2\sigma_0, \quad \sigma_{00} < \sigma. \tag{52}$$

Moreover, an exact solution for a ST corner soliton can be found too:

$$U_{m,n} = A(-1)^n \exp\left(-\frac{\alpha}{2}(m+n)\right), \tag{53}$$

$$A^2 = (\sigma_{00} - \sigma)^{-1} \exp\left(\frac{\alpha}{2}\right), \quad K = -2 \cosh\left(\frac{\alpha}{2}\right) - 2 - \sigma A^2. \tag{54}$$

In the latter case, the additional condition is opposite to that given by Eq. (52) for the UnST mode:

$$\sigma + \sigma_{00} = 2\sigma_0, \sigma < \sigma_{00}. \quad (55)$$

The 2D system will be considered in detail elsewhere.

Acknowledgments

G.G., A.M., and Lj.H. acknowledge support from the Ministry of Education, Science and Technological Development of the Republic of Serbia (Project III45010). B.A.M. appreciates a valuable discussion with Y. V. Kartashov, and hospitality of the Vinča Institute (Belgrade).

-
- [1] Y. S. Kivshar and G. P. Agrawal, *Optical Solitons: From Fibers to Photonic Crystals* (Academic, San Diego, CA, 2003).
- [2] V. A. Brazhnyi and V. V. Konotop, *Mod. Phys. Lett. B* **18**, 627 (2004); O. Morsch and M. Oberthaler, *Rev. Mod. Phys.* **78**, 179 (2006).
- [3] L. Torner, *IEEE Photonics Technol. Lett.* **11**, 1268 (1999); I. Towers and B. A. Malomed, *J. Opt. Soc. Am.* **19**, 537 (2002); F. K. Abdullaev, J. G. Caputo, R. A. Kraenkel, and B. A. Malomed, *Phys. Rev. A* **67**, 013605 (2003); H. Saito and M. Ueda, *Phys. Rev. Lett.* **90**, 040403 (2003).
- [4] Y. V. Kartashov, B. A. Malomed, and L. Torner, *Rev. Mod. Phys.* **83**, 247 (2011).
- [5] O. V. Borovkova, Y. V. Kartashov, B. A. Malomed, and L. Torner, *Opt. Lett.* **36**, 3088 (2011);
- [6] O. V. Borovkova, Y. V. Kartashov, L. Torner, and B. A. Malomed, *Phys. Rev. E* **84**, 035602 (R) (2011).
- [7] J. Zeng and B. A. Malomed, *Phys. Rev. E* **86**, 036607 (2012).
- [8] Y. He and B. A. Malomed, *Phys. Rev. A* **87**, 053812 (2013).
- [9] W.-P. Zhong, M. Belić, G. Assanto, B. A. Malomed, and T. Huang, *Phys. Rev. A* **84**, 043801 (2011).
- [10] J. Hukriede, D. Runde, and D. Kip, *J. Phys. D* **36**, R1 (2003).
- [11] P. O. Fedichev, Y. Kagan, G. V. Shlyapnikov, and J. T. M. Walraven, *Phys. Rev. Lett.* **77**, 2913 (1996); S. Inouye, M. R. Andrews, J. Stenger, H. J. Miesner, D. M. Stamper-Kurn, and W. Ketterle, *Nature (London)* **392**, 151 (1998); M. Theis, G. Thalhammer, K. Winkler, M. Hellwig, G. Ruff, R. Grimm, and J. H. Denschlag, *ibid.* **93**, 123001 (2004).
- [12] I. Bloch, J. Dalibard, and W. Zwerger, *Rev. Mod. Phys.* **80**, 885 (2008); C. Chin, R. Grimm, P. Julienne, and E. Tiesinga, *ibid.* **82**, 1225 (2010).
- [13] W. L. Barnes, A. Dereux, and T. W. Ebbesen, *Nature* **424**, 824 (2003).
- [14] P. G. Kevrekidis, *The Discrete Nonlinear Schrödinger Equation: Mathematical Analysis, Numerical Computations, and Physical Perspectives* (Springer: Berlin and Heidelberg, 2009).
- [15] S. G. Davison and M. Steslicka, *Basic Theory of Surface States* (Oxford, 1992).
- [16] I. E. Tamm, *Z. Phys.* **76**, 849 (1932).
- [17] M. I. Molina, R. A. Vicencio, Yu. S. Kivshar, *Optics Letters* **31**, 1693 (2006).
- [18] M. Miyagi and S. Nishida, *Sci. Rep. Res. Inst. Tohoku Univ. Ser. B* **24**, 53 (1972).
- [19] K. G. Markis, S. Suntsov, D. N. Christodoulides, G. I. Stegeman, and A. Hache, *Opt. Lett.* **30**, 2466 (2005).
- [20] Yu. S. Kivshar and D. K. Campbell, *Phys. Rev. E* **48**, 3077 (1993).
- [21] Lj. Hadžieski, A. Maluckov, M. Stepić, and D. Kip, *Phys. Rev. Lett.* **93**, 033901 (2004).
- [22] S. Darmanyan, A. Kobayakov, and F. Lederer, *J. Exp. Theor. Phys.* **86**, 682 (1998).
- [23] A. Maluckov, Lj. Hadžievski, B. A. Malomed, L. Salasnich, *Phys. Rev. A* **78**, 013616 (2008).
- [24] B. Malomed and M. Weinstein, *Phys. Lett. A* **220**, 91 (1996); D. J. Kaup, *Math. Comput. Simul.* **69**, 322 (2005); R. Carretero-González, J. D. Talley, C. Chong, and B. A. Malomed, *Physica D* **216**, 77 (2006); C. Chong, R. Carretero-González, B. A. Malomed, and P. G. Kevrekidis, *ibid.* **238**, 126 (2009); C. Chong, D. E. Pelinovsky, and G. Schneider, *Physica D* **241**, 115 (2011); B. A. Malomed, D. J. Kaup, and R. A. Van Gorder, *Phys. Rev. E* **85**, 026604 (2012).
- [25] G. Herring, P. G. Kevrekidis, B. A. Malomed, R. Carretero-González, and D. J. Frantzeskakis, *Phys. Rev. E* **76**, 066606 (2007).
- [26] Lj. Hadžievski, G. Gligorić, A. Maluckov, and B. A. Malomed, *Phys. Rev. A* **82**, 033806 (2010); M. D. Petrović, G. Gligorić, A. Maluckov, Lj. Hadžievski, and B. A. Malomed, *Phys. Rev. E* **84**, 026602 (2011); M. Stojanović, A. Maluckov, Lj. Hadžievski, and B. A. Malomed, *Physica D* **240**, 1489 (2011).
- [27] R. Blit and B. A. Malomed, *Phys. Rev. A* **86**, 043841 (2012).
- [28] X. Shi, F. Ye, B. Malomed, and X. Chen, *Nonlinear surface lattice coupler*, *Opt. Lett.* **38**, in press.
- [29] X. S. Wang, A. Bezryadina, Z. G. Chen, K. G. Makris, D. N. Christodoulides, and G. I. Stegeman, *Phys. Rev. Lett.* **98**, 123903 (2007); D. Mihalache, D. Mazilu, F. Lederer, and Y. S. Kivshar, *Opt. Lett.* **32**, 3173 (2007); R. A. Vicencio, S. Flach, M. I. Molina, and Y. S. Kivshar, *Phys. Lett. A* **364**, 274 (2007); Y. V. Bludov and V. V. Konotop, *Phys. Rev. E* **76**, 046604 (2007); D. Mihalache and D. Mazilu, *Romanian Rep. Phys.* **61**, 235 (2009); M. I. Molina and Y. S. Kivshar, *J. Opt. Soc. Am. B* **26**, 1545 (2009); M. Heinrich, Y. V. Kartashov, A. Szameit, F. Dreisow, R. Keil, S. Nolte, A. Tünnermann, V. A. Vysloukh, and L. Torner, *Opt. Lett.* **34**, 1624 (2009); D. Jović, C. Denz, and M. Belić, *Opt. Exp.* **19**, 26232 (2011).